Journal of Solid State Chemistry **167,** 302–309 (2002)
doi:10.1006/jssc.2002.9648

Host–Guest Interactions and Laser Activity in $AlPO_4$-5/Laser Dye Composites

Ö. Weiß, J. Loerke, U. Wüstefeld, F. Marlow, and F. Schüth[1]

Max-Planck-Institut für Kohlenforschung, Kaiser-Wilhelm-Platz, 1 Mülheim an der Ruhr D-45470 Germany

Received November 14, 2001; in revised form April 30, 2002; accepted May 10, 2002

IN HONOR OF PROFESSOR GALEN STUCKY ON THE OCCASION OF HIS 65TH BIRTHDAY

***In situ* inclusion of the laser dyes coumarin 466, coumarin 7, pyridine 2 and DCM has been conducted successfully in $AlPO_4$-5 crystals. The charged molecule pyridine 2 interacts with the framework and leads to bundle-like morphologies with increasing dye content. Uncharged molecules (DCM, coumarin 7, coumarin 466) are included, although corresponding molecular dimensions are exceeding pore size. These dyes probably induce local defects in the pore walls of $AlPO_4$-5 which are healed during crystal growth leading to well-developed hexagonal prisms. Spectroscopic studies show interactions of the dyes with the solid-state matrix which are reflected by shifts of absorption and emission maxima of the dyes. For the first time, laser activity is demonstrated on a perfect hexagonal single $AlPO_4$-5/DCM crystal.** © 2002 Elsevier Science (USA)

***Key Words: in situ* inclusion; $AlPO_4$-5; laser dyes; host–guest interaction; laser activity.**

INTRODUCTION

New possible application fields for zeolites and zeolite-type aluminophosphates have been intensively studied in the last decade of the 20th century. New materials based on molecular sieve compounds attracted high attention and their synthesis and characterization was a new challenge in microporous and mesoporous materials science (1–4). Molecular sieves allow the inclusion of a variety of guest molecules. The defined pore system can act as an ordering framework for the included species which leads to materials with new, e.g., non-linear optical properties. Another decisive point is the possibility to modify properties of either the guest molecule or the host framework independently. Following the route of incorporating guest species in the channel system of zeolites and aluminophosphates, it was possible to realize new supramolecular structures with interesting functions. These include molecular sieve based phosphors (5, 6), frequency doublers (7), optical switches (8), pigments (9) and lasers (10).

Lasing from a modified molecular sieve was for the first time demonstrated with $AlPO_4$-5/pyridine 2 crystals (11, 12). The laser action from the central part is characterized by a *whispering gallery mode* caused by total internal reflection of the propagating light at the hexagonal sides leading to amplification. The first microlaser materials, however, only had a perfect center, but defective crystal ends which triggered work to develop a synthesis strategy yielding $AlPO_4$-5 crystals with perfect hexagonal morphology and crystal sizes up to 1 mm (13). $AlPO_4$-5 crystals acting as microcavities determine the resonator type, and the large size and perfect morphology eases spectroscopic characterization on single crystals. Independently of the laser active molecule, modification of the resonator can be realized by changing crystal size and structure type. With a smaller crystal size, the dimensions of the resonator are also decreased, which results in lower lasing thresholds (14).

We focus in this study on large well-developed laser dye loaded $AlPO_4$-5 crystals, the host–guest interaction during crystallization of the composite and the influence of the host lattice on the spectroscopic properties of the guest molecule. We present data on synthesis series with laser dyes differing in molecule size and functionality. Spectral information on the composites is obtained from single crystal studies giving direct and local information. Laser activity is demonstrated on single $AlPO_4$-5/DCM crystals with perfect hexagonal morphology.

EXPERIMENTAL

As laser dyes we chose 7-diethylaminocoumarine (trade name: coumarine 466), 3-(2′-benzimidazoyl)-7-*N,N*-diethylaminocoumarine (trade name: coumarine 7), 1-ethyl-4-(4-(*p* - dimethylaminophenyl) - 1,3 - butadienyl) - pyridinium Perchlorat (trade name: pyridine 2) and 4-dicyanmethy-

[1]To whom correspondence should be addressed. Fax: +49-208-306-2995. E-mail: schueth@mpi-muelheim.mpg.de.

0022-4596/02 $35.00

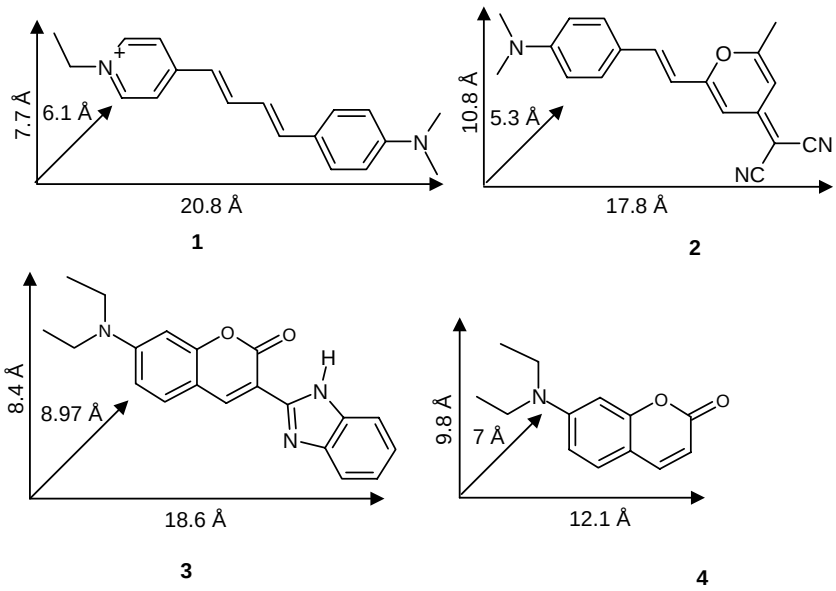

FIG. 1. Van der Waals dimensions and molecular structures of the laser dyes pyridine 2 (**1**), DCM (**2**), coumarin 7 (**3**) and coumarin 466 (**4**).

lene-2-methyl-6-(*p*-dimethylaminostyryl)-4*H*-pyran (trade name: DCM).

The synthesis of $AlPO_4$-5/dye-composites was based on the procedure for $AlPO_4$-5 synthesis as reported before (13) with additional adding of the laser dyes which were dissolved in ethanol. The synthesis gel was prepared as follows: orthophosphoric acid (Fluka), ultrapurified water (Millipore) and tripropylamine (TPA, Aldrich) were combined (solution A) and cooled down to 279 K. The organic laser dye, ethanol (EtOH) and our laboratory-made $Al(OH)_3$ precursor (15) were combined (solution B) and stirred for 15 min. Solution A was added dropwise to solution B over a period of 10 min followed by a final stirring of 15 min. The synthesis gel was filled into PTFE-lined autoclaves which were then placed into a preheated heating block. The crystallization time was normally 16–20 h at 453 K. The standard molar gel composition was 1 Al_2O_3:1.03 P_2O_5:1.78 TPA:750 H_2O:27.6 EtOH:x dye, whereas x was varied, depending on the dye, between 0.067 and 0.019. All synthesis products were separated by threefold decanting, washing and drying at 363 K overnight.

Optical spectra on single crystals were recorded with a Leica MPV-SP UV/Vis microscope spectrometer. Samples were embedded in synthetic canada balsam. This minimizes scattering at the surface and eases handling of the samples. Fluorescence spectra were recorded on powder samples. Photographs of the fluorescing crystals were taken with a camera connected to the Leica microscope. To study laser activity, single crystals were mounted with their end face on a glass plate and excited with 10 ns pulses from a frequency-doubled Nd:YAG laser (Spectron Laser Systems SL-456) at a wavelength of 532 nm. A rectangular section with a uniform intensity distribution (2 mm × 3 mm) was cut from the middle of the laser beam with the help of a variable slit and imaged onto the sample producing a stripe of excitation light along the crystals length axis (3 mm × 600 μm). The light emitted from the crystal was imaged onto the entrance slit of a monochromator (Acton Research SpectraPro 500) and detected by a nitrogen-cooled CCD (Princeton Instruments LN/CCD 1100).

Calculations of molecular dimensions were performed with the program Titan (Wavefunction Inc.). The structures were optimized by semiempirical PM3 calculations starting from a preoptimized MMFF structure giving geometrical dimensions.

RESULTS AND DISCUSSION

The dyes were chosen in order to study the influence of their spatial dimensions and their chemical functionality on the incorporation behavior and on the morphology of the synthesized crystals. The effects of (*a*) *a charged slim molecule* (*pyridine 2*) and (*b*) *uncharged molecules that exceed the channel size* (DCM, coumarin 466, coumarin 7) were studied in syntheses with increasing dye concentration in the synthesis gel. In Fig. 1 the van der Waals dimensions of the molecules are shown.

Morphology of $AlPO_4$-5/Laser Dye Composites

In Fig. 2 photographs of fluorescing $AlPO_4$-5 crystals loaded with coumarin 466, coumarin 7, pyridine 2, and DCM are shown. All *in situ* inclusion syntheses were

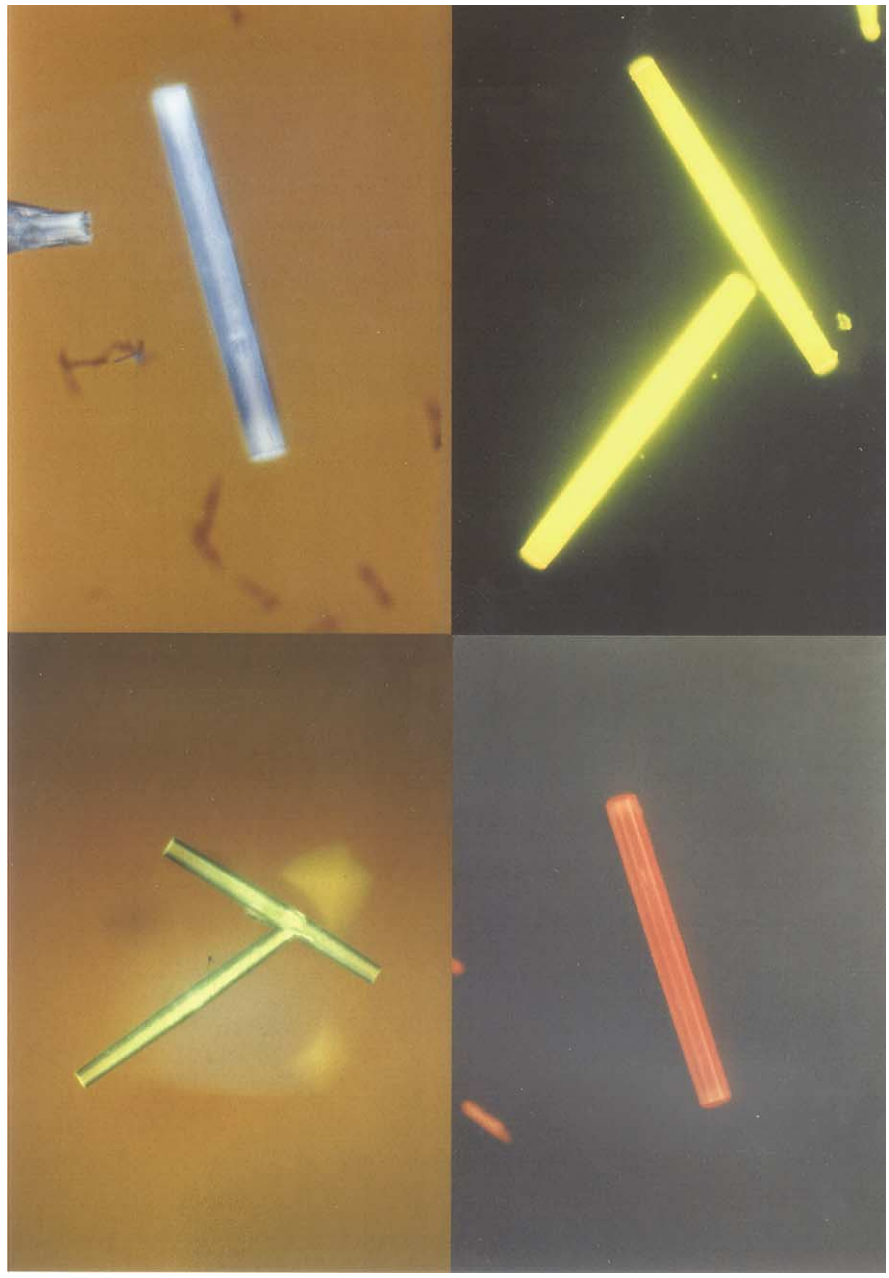

FIG. 2. Fluorescing $AlPO_4$-5/laser dye crystals: $AlPO_4$-5/coumarin 466 (blue), $AlPO_4$-5/coumarin 7 (green), $AlPO_4$-5/DCM (yellow), $AlPO_4$-5/pyridine 2 (red).

successful, the dyes can be incorporated in the $AlPO_4$-5 structure. As coumarin 466 and coumarin 7 absorb light below 450 nm, the crystals appear only slightly yellow, crystals loaded with pyridine 2 are dark red and those synthesized with DCM are orange in color. The fluorescence, visible for all materials, however, is much more characteristic.

The proof that the dye is located in the pore system is given by exciting the crystals with polarized light (Fig. 3). The crystals only absorb light polarized parallel to the crystals long axis. The transition dipole moment of these dyes is basically parallel to the long axis of the molecules. The polarized absorption parallel to the crystal *c*-axis, i.e., in the direction of the channels, thus means that the dye molecules are aligned in the channel direction. This would not be possible for dyes adsorbed on the external surface or in large mesopores. Adsorption in small mesopores/large micropores having the same orientational relationship to

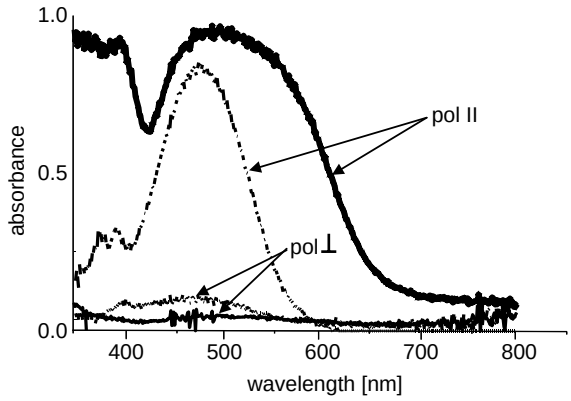

FIG. 3. Polarized absorption spectra of single $AlPO_4$-5/ pyridine 2 (solid line) and DCM/ $AlPO_4$-5 crystals (dashed line).

the morphology of the crystals as the channels, however, would also explain the polarized absorption observed on $AlPO_4$-5/DCM crystals.

The results obtained upon increasing the concentration of pyridine 2, DCM and coumarin 7 in the synthesis gel are summarized in Table 1. Syntheses in the presence of coumarin 466, coumarin 7 and DCM gave similar results concerning crystal quality and morphology. An increase of the dye concentration in the synthesis gel for DCM and coumarin 7 did not severely affect morphologies. Crystals achieve a maximum length of up to 0.7 mm and have perfect hexagonal shape. The fraction of perfect and distorted crystals is comparable to that found in the synthesis of pure $AlPO_4$-5 (13), but here all crystals are loaded with dye. The presence of pyridine 2 in the synthesis gel, however, leads to an extreme reduction of the fraction of perfect crystals. Most of the crystals are highly loaded but show bundle-like shapes except for the central part (11) or are intergrown. This effect is also strongly dependent on the dye offer as increasing concentration of pyridine 2 in the synthesis gel leads to a decrease of the fraction of perfect hexagonal crystals. A dye concentration of 5.9×10^{-4} mol/L (corresponding to an Al_2O_3/dye molar ratio of 0.01) in the synthesis gel already leads to a very low fraction of hexagonal prisms with lengths up to 0.5 mm. Above a concentration of 8.8×10^{-4} mol/L (corresponding to an Al_2O_3/dye molar ratio of 0.016), all crystals show the bundle-like morphology and single crystal studies are not possible any more. Thus, the pyridine 2 concentration was not increased further.

TABLE 1
Results of Synthesis Series with Coumarin 466, Coumarin 7, Pyridine 2, and DCM

No.	Laser dye	Al2O3/dye ratio	Dye concentration/wt%	Crystal morphology[a]
A	Coumarin 466		Not detectable	h
B	Coumarin 7	0.0067	Not detectable	h
C		0.0085	Not detectable	h
D		0.01	Not detectable	h
E	Pyridine 2	0.01	0.13[b]	h, b
F		0.013	0.19[c]	b, h
G		0.016	Not detectable	b
H	DCM	0.01	0.03[b]	h
J		0.013	0.04[b]	h
K		0.016	0.05[b]	h
L		0.019	0.07[b]	h

[a] h = hexagonal prisms, b = bundle-like.
[b] Middle section of the crystals corresponding to position 3.
[c] End section of crystals corresponding to positions 1 and 5.

Nevertheless, compared to earlier results where syntheses have been carried out with TEA (11), the use of TPA as template generally results in better quality of the crystals, especially in the case of pyridine 2. It is possible to prolong the crystallization time up to 16 h which is in contrast to earlier syntheses where crystallization times could not exceed 1 h without affecting crystal morphology. This modification allows to increase the size of $AlPO_4$-5/pyridine 2 composite crystals to up to 0.5 mm.

The diffraction pattern of the products obtained in the presence of coumarins and DCM proved that the dye additions did not change the phase composition. All syntheses yielded $AlPO_4$-5 and the well-known dense by products as observed before in $AlPO_4$-5 synthesis (13). Syntheses carried out with pyridine 2 resulted in the formation of pure $AlPO_4$-5, but the drastically changed morphologies indicate the strong influence of this dye.

The influence of the different dyes on the morphology of the crystals is pronounced and may be understood as follows: For the templated growth of porous solids the template has a crucial role, since it directs the structure, but may also strongly influence the crystal morphologies or element distribution in the crystals. As the aluminophosphate network has no net charge, the tertiary amines normally used as template molecules are occluded as hydroxide salts (16, 17). The resulting tripropylammonium cations interact with the aluminophosphate framework via hydrogen bonding, while the hydroxide ions coordinate framework aluminium atoms, causing a distorted five fold coordination. Synthesis of $AlPO_4$-5 with TPA instead of TEA results in a lowered interaction of the alkylammonium ion with the pore walls. This is due to the orientation of the trialkyl groups which form a tripod shielding the ammonium position and the hydroxide ion (18). The interaction of the template with the framework will thus be low. Additional species with ammonium-functionality which is not shielded, such as pyridine 2 with the pyridinium-position, will have stronger interactions with the framework. It can then be envisaged that this would lead to a disturbed growth of the crystals. Although there is no direct evidence for this hypothesis, it is supported by the

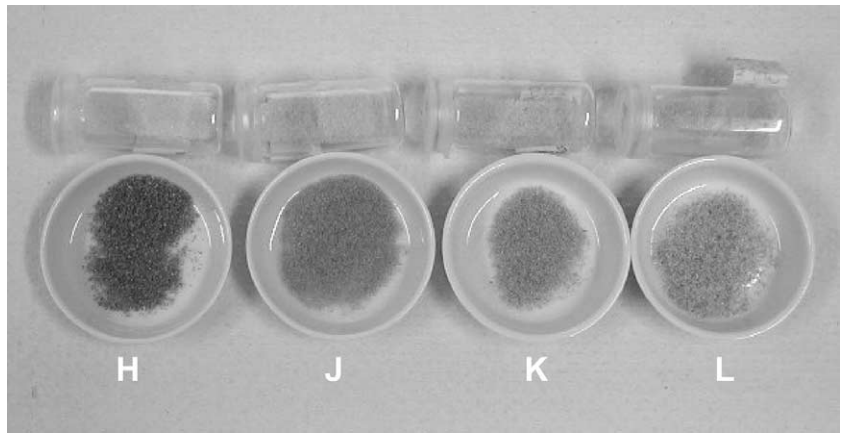

FIG. 4. $AlPO_4$-5/DCM syntheses results. Intensity of color of as-made crystals and corresponding calcined crystals (samples H–L).

fact that only the presence of pyridine 2 leads to disturbed crystal growth, which is amplified at higher concentration of the dye, but the uncharged other dye molecules do not lead to changes in the morphology.

In order to fit the larger dye molecules into the pore system, local defects have to be found to accommodate the guest species. Using uncharged molecules like the coumarins and DCM, Coulomb interactions with the framework are minimized and the van der Waals fit in the pore is expected to play the key role. However, DCM and the coumarins exceed the pore size of $AlPO_4$-5, but nevertheless are incorporated aligned in the channels, while the crystals retain their rather perfect hexagonal morphology. Aligned incorporation is only possible if defects are induced and pore sizes are increased to accommodate the dye molecules. The defect positions could be located in the pore walls easing the dye molecules to align in the channel. An indication that such defects form which influence the accessibility of the channel system is given by the calcination behavior of the loaded crystals. $AlPO_4$-5 is notoriously difficult to calcine since the unidimensional channel system is easily blocked, especially for large crystals. With DCM, it was observed that the brown coloration developed after calcination at 873 K in air is much less pronounced with higher dye incorporation, which suggests the presence of additional pores, facilitating mass transfer (Fig. 4). These additional pores, however, have to be rather small, since they cannot be discriminated from the micropores in nitrogen sorption experiments. Also their concentration is difficult to assess, since for large $AlPO_4$-5 crystals the pore system is never fully accessible due to channel blocking by faults in the structure. Increasing dye concentration typically led to increasing pore volume in the calcined crystals, but this is due both to the additional non-structural pores and to the improved accessibility of the structural pores.

Dye Loading Levels and Profiles

Polarized absorption spectra recorded along the crystals' *c*-axis with a measuring spot size of about $10 \times 10\,\mu m^2$ give information on the loading profiles of the $AlPO_4$-5 crystals. For each batch, several crystals were examined to gain representative data. For sample F, no crystals with perfect overall morphology were present. For these crystals, therefore, the end sections were analyzed, which were at least locally perfectly hexagonal and thus allowed to record spectra which were unperturbed by scattering. The dye content was determined by the method introduced in (19), according to calculations based on the Beer–Lambert Law.

Loading levels in $AlPO_4$-5/coumarin 7 are so low that studies on single crystals were not possible. The absorption spectra do not exhibit a maximum which would allow the calculation of dye concentrations to gain quantitative data on dye loadings. When powder samples are excited at 433 nm, however, corresponding to data for the absorption band in ethanol (20), samples B–D exhibit a fluorescence maximum at around 480 nm, the intensity of which increases which increasing dye concentration in the synthesis gel (Fig. 5). The increasing luminescence intensity thus gives indirect evidence for a higher concentration of coumarin 7 in $AlPO_4$-5 with increasing dye offer.

Pyridine-2- and DCM-loaded crystals show an increased absorption with increasing dye concentration in the crystals (Figs. 6 and 7). The corresponding dye contents are summarized in Table 1. Studies on single crystals along the crystals' *c*-axis give information on the dye content profile. Dye concentrations in pyridine-2- and DCM-loaded $AlPO_4$-5 crystals are high in the middle of the crystals decreasing towards either ends. This profile could be detected in all crystals analyzed and is shown in Fig. 8 in comparison for pyridine 2 and DCM. The same concentration of dye in the synthesis gel leads to an 11 times

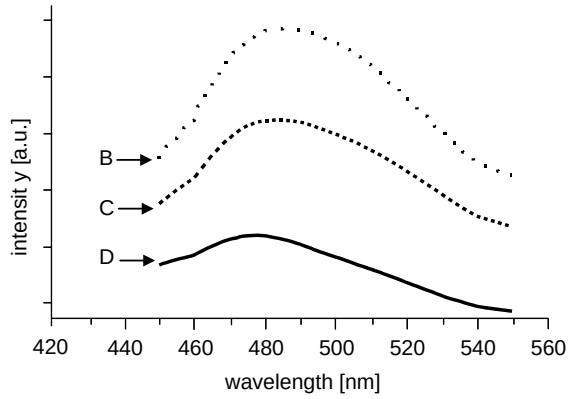

FIG. 5. Fluorescence spectra of $AlPO_4$-5/coumarin 7 crystals with increasing dye content.

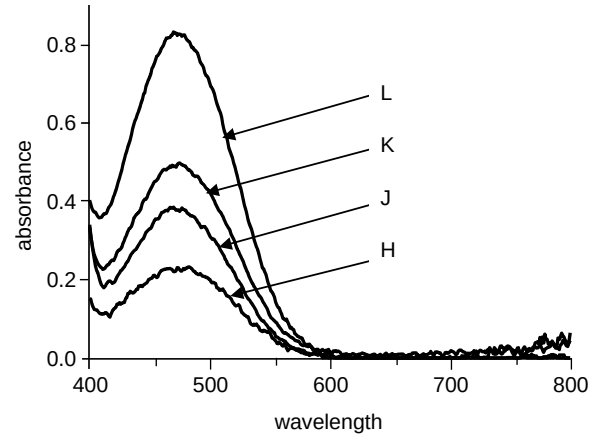

FIG. 7. Absorption spectra of single $AlPO_4$-5/DCM crystals (samples H–L) with increasing dye content.

higher concentration of pyridine 2 in the crystal compared to DCM.

The higher loading profiles of $AlPO_4$-5/pyridine 2 composites show again the stronger interaction of the charged pyridine 2 with the matrix and also reflects the fact that the size of the molecule is more favorable with respect to incorporation in the channels. Nevertheless, it is possible to incorporate molecules which are exceeding the pore size. The inhomogeneous loading profiles are an indication that incorporation rates are very high in the early stages of crystal growth, since these crystals start to grow from the center to both sides. It can be summarized that in all series an increasing dye uptake with increasing dye concentration in the gel was observed, the highest loading levels being achieved with pyridine 2.

From these studies, it is evident that in order to generate new laser materials, based on the combination of molecular sieves with organic laser dyes, two opposing treads have to be considered: High loading levels which are advantageous for laser operation are possible by using charged molecules. However, adjusting dye concentration is difficult as these dyes show strong interaction with the growing crystal and the resonator geometry will be distorted. This problem can be solved by using uncharged molecules which, however, lead to a lower degree of incorporation.

Host Influence on Laser Dyes

Absorption spectra of $AlPO_4$-5/pyridine composites show a maximum at about 500 nm corresponding to the data measured in ethanol (20). In contrast to spectra in solution, where an additional absorption band is detected at 320 nm, this band is shifted to 380 nm in $AlPO_4$-5 (Fig. 6). $AlPO_4$-5/DCM spectra show an absorption band at 472 nm (Fig. 7). An additional small absorption in the UV region centered at about 370 nm could be due to the presence of the *cis*-isomer as discussed in (21).

$AlPO_4$-5 crystals provide a polar environment originating from a partial positive charge at the aluminum and a

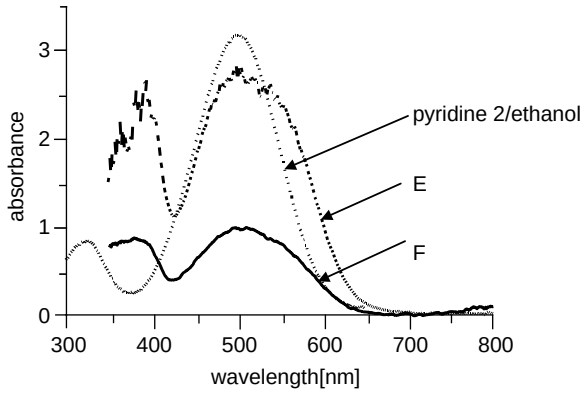

FIG. 6. Absorption spectra of single $AlPO_4$-5/pyridine 2 crystals (samples E and F) with increasing dye content.

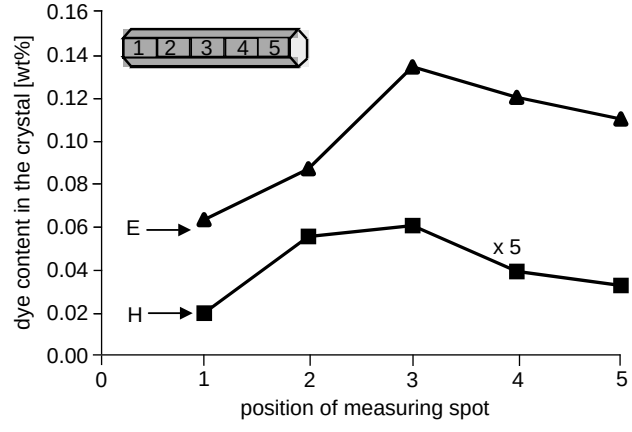

FIG. 8. Dye contents in single crystals from samples of synthesis E and H. Scheme indicating principle of measuring position.

less positive charge at the phosphorus atoms of the framework. Therefore, dipole–dipole interactions with the dye molecule would lower polar states in energy, which are typically the excited states for the dyes investigated.

As the energy-level diagram of pyridine 2 is not known, the origin for this absorption can only be assumed. The unaffected main band should correspond to a π,π^* transition. A dipole moment of the excited state which is not differing significantly from the ground state could be an explanation for the fact that this band is not shifted. The shift of the other absorption band to around 380 nm compared to solution at 320 nm could be caused by an increase of the dipole moment of the excited state which would thus be lowered in energy by the host-lattice.

DCM is a solvatochromic molecule, so that from spectral shifts conclusions concerning polarity of the surrounding media can be drawn (22). The absorption maximum at 472 nm corresponds to an internal charge transfer process (23) and is not shifted compared to ethanol as polar solvent but blue shifted compared to an unpolar solvent such a $CHCl_3$. From this observation, we conclude that the dipole–dipole interactions during the absorption process of the $AlPO_4$-5 lattice with DCM are similar to those of ethanol with DCM. In contrast to that fluorescence is blue shifted compared to spectra in ethanol decreasing the stokes shift from 172 nm in ethanol to 106 nm in $AlPO_4$-5 (Fig. 9) and red shifted compared to the unpolar solvent $CHCl_3$. To explain this observation, it has to be considered that: (i) the dipole moment of the excited state S_1 ($\mu = 26.3$ D) is much larger than the ground state S_0 ($\mu = 6.1$ D) (23) and (ii) that the $AlPO_4$-5 framework is rigid while the ethanol molecules can reorientate. A more polar state S_1 will be lowered in energy in ethanol due to reorientation of the solvent molecules and higher solvatation of the exited state. In the non-polar solvent $CHCl_3$, the interaction of the solvent molecules with the excited state is low so that the excited state is basically unaffected (blue shift with respect to ethanol). In $AlPO_4$-5, the excited state is lowered to some extent by the polar framework, but since this polar environment is rigid, the stabilization would be less pronounced (red shift with respect to $CHCl_3$) than in ethanol which can adopt by reorientation to the polarity of the excited state (stronger red shift with respect to $CHCl_3$).

Laser Activity in $AlPO_4$-5/DCM Crystals

In general, a strong overlapping region is undesired for laser dyes. Nevertheless, efficient laser emission from $AlPO_4$-5/DCM crystals has been detected. In contrast to our earlier experiments with $AlPO_4$-5/pyridine 2, where lasing crystals were always intergrown and showed distorted morphologies, for the first time laser emission from a large, perfect rod-like, hexagonally shaped crystal is demonstrated. Exciting a single crystal with the second harmonic of a Nd–YAG laser leads to the laser emission spectrum shown in Fig. 10. Spectral spikes are detected in the region of 605–635 nm with a discrete line spacing indicating the mode propagating in the hexagonal cavity. Laser emission is in the orange-red spectral range since reabsorption losses, which are noticeable up to 600 nm, and wavelength-dependent scattering losses modify the gain spectrum slightly compared to the fluorescence. The background is low compared to the intensity of the spectral lines which suggest that losses due to non-amplified emission are low. The expected wavelength spacing of the modes reflects the size of the resonator. The size of the resonator in the studied crystal can be expressed by the distances d of the opposite sides. As the hexagon was slightly skewed, an average distance was used for the determination.

According to calculations described in (14), the resonator size which relates to the distance d can be calculated from the line spacing of the different laser modes:

$$d = \frac{\lambda_0^2}{3\Delta\lambda_0 n_{\mathrm{AlPO_4\text{-}5}}}$$

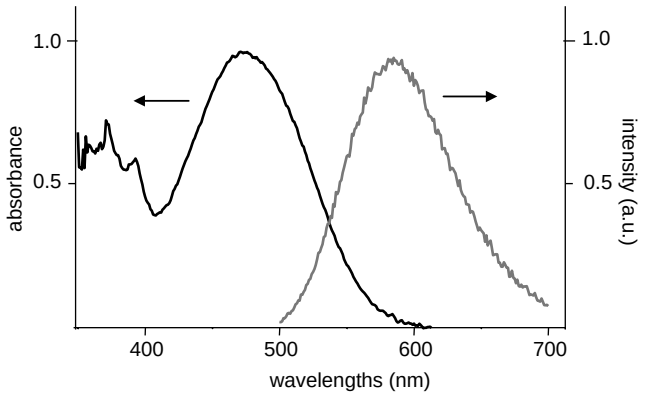

FIG. 9. Absorption and emission spectra of $AlPO_4$-5/DCM crystals showing overlapping region.

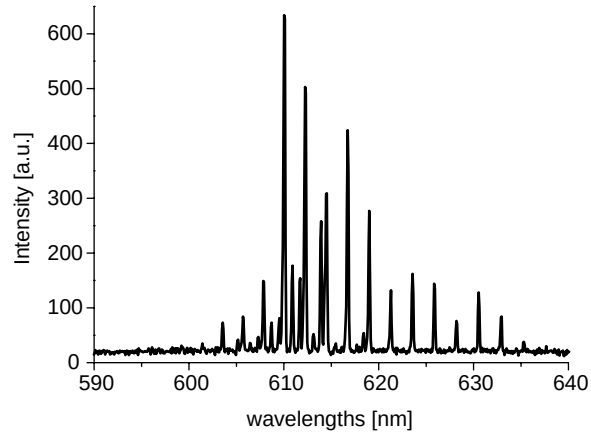

FIG. 10. Laser emission spectra of a single $AlPO_4$-5/DCM crystal.

The observed line spacing of 2.26 nm thus corresponds to a distance of 38.7 μm, which is in the range of the microscopically obtained distance of 28.4 μm investigated in this particular case. The deviation could be a result of errors in the determination of the distance d from micrographs and of the fact that the refractive index is modified due to the presence of the dye molecules. Although the dye concentration is low, the effect on the refractive index could be significant because the laser operation wavelength is very close to the molecular transitions.

CONCLUSIONS

In situ inclusion of dye molecules differing in size and functionality in $AlPO_4$-5 crystals has been conducted successfully. The following has been observed:

(a) Uncharged laser dye molecules, such as coumarin 466, coumarin 7 and DCM do not affect crystal morphology.

(b) The strong interactions of the charged molecule pyridine 2, which should fit into the pore, with the $AlPO_4$-5 framework results in strongly distorted crystal growth, but also a high uptake of dye.

(c) The uncharged molecule DCM, which exceeds pore dimensions of $AlPO_4$-5, is aligned, which means that it induces defects in the pore walls to be accomodated. The solvatochromic nature of the molecule is reflected well in the absorption and emission spectra, indicating the strong host–guest interactions.

(d) Perfect hexagonal $AlPO_4$-5/DCM crystals show a pronounced laser activity although dye loading levels are low compared to pyridine 2.

ACKNOWLEDGMENTS

We would like to thank F. Laeri for fruitful discussions. This work was founded by the DFG under Grant SCHU 744/10-2.

REFERENCES

1. G. D. Stucky and I. McDougall, *Science* **247,** 669 (1990).
2. G. A. Ozin, *Adv. Mater.* **4,** 612–649 (1992).
3. J. Sauer, F. Marlow, and F. Schüth, in "Handbook of Advanced Electronic and Photonic Materials and Devices," (H. S. Nalwa Ed.), Vol. 6. Academic Press, London, 2001.
4. R. C. Hayward, P. Alberius-Henning, B. F. Chmelka, and G. D Stucky, *Microporous Mesoporous Mater.* **44,** 619–624 (2001).
5. M. Bredol, U. Kynast, and C. Ronda, *Adv. Mater.* **3,** 361 (1991).
6. C. Borgmann, J. Sauer, T. Jüstel, U. Kynast, and F. Schüth, *Adv. Mater.* **11,** 45–49 (1999).
7. F. Marlow, J. Caro, L. Werner, J. Kornatowski, and S. Dähne, *J. Phys. Chem.* **97,** 11,286 (1993).
8. K. Hoffman, F. Marlow, and J. Caro, *Adv. Mater.* **9,** 567 (1997).
9. M. Bockstette, D. Wöhrle, I. Braun, and G. Schulz-Ekloff, *Microporous Mesoporous Mater.* **23,** 83–96 (1998).
10. F. Marlow, M. D. McGehee, D. Y. Zhao, B. F. Chmelka, and G. D. Stucky, *Adv. Mater.* **11,** 632 (1999).
11. G. Ihlein, F. Schüth, O. Krauß, U. Vietze, and F. Laeri, *Adv. Mater.* **10,** 1117 (1998).
12. U. Vietze, O. Krauß, F. Laeri, G. Ihlein, F. Schüth, and B. Limburg, *Phys. Rev. Lett.* **81,** 4628 (1998).
13. Ö. Weiß, G. Ihlein, and F. Schüth, *Microporous Mesoporous Mater.* **35–36,** 617 (2000).
14. I. Braun, G. Ihlein, F. Laeri, J. Nöckel, G. Schulz-Ekloff, F. Schüth, U. Vietze, Ö. Weiß, and D. Wöhrle, *Appl. Phys. B* **70,** 335 (2000).
15. S. Schunk, D. G. Demuth, B. Schulz-Dobrick, K. K. Unger, and F. Schüth, *Microporous Mater.* **6,** 273 (1996).
16. K. H. Schnabel, G. Finger, J. Kornatowski, E. Loeffler, C. Peuker, and W. Pilz, *Microporous Mater.* **11,** 293 (1997).
17. S. Popescu, S. Thomson, and R. F. Howe, *Phys. Chem. Chem. Phys.* **3,** 111–118 (2001).
18. J. M. Bennett, J. P. Cohen, and E. M. Flanigen, *in* "Intrazeolite Chemistry" (G. D. Stucky, F. G. Dwyer, Eds.), "ACS Symposium Series," Vol. 218, p. 109. ACS, Washington DC, (1983).
19. K. Hoffmann, F. Marlow, and J. Caro, *Zeolites*, **16,** 281 (1995).
20. U. Brackmann, "Lambdachrome Laser Dyes." Lambda Physik GmbH, Göttingen, 1985.
21. Ö. Weiss, F. Schüth, l. Benmohammadi, and F. Laeri, *Stud. Surf. Sci. Catal.* **135,** 21-O-04 (on CD).
22. C. Reichardt, "Solvents and Solvent Effects in Organic Chemistry." VCH, Weinheim, 1988.
23. M. Meyer and J. C. Mialocq, *Opt. Commun* **64,** 264 (1987).